AIAA JOURNAL
Vol. 38, No. 10, October 2000

Technical Notes

TECHNICAL NOTES are short manuscripts describing new developments or important results of a preliminary nature. These Notes cannot exceed six manuscript pages and three figures; a page of text may be substituted for a figure and vice versa. After informal review by the editors, they may be published within a few months of the date of receipt. Style requirements are the same as for regular contributions (see inside back cover).

Convergence Acceleration of an Inverse Design Technique for Constructing Turbomachinery Cascades

Jeffrey W. Yokota* and Adam J. Medd‡
University of Alberta, Edmonton, Alberta T6G 2G8, Canada

I. Introduction

WITH this work we present several new ways to accelerate the convergence of an inverse design technique for constructing transonic turbomachinery cascades. This work is based on the inverse design theories of Hawthorne et al.[1] and Tan et al.,[2] in general, and Dang,[3] in particular.

In Dang's method[3] a compressible finite volume scheme is used to construct the flow around a blade whose geometry is designed to match a prescribed flow turning distribution. The blade geometry is decomposed into a prescribed thickness distribution and a camberline, the shape of which is obtained, iteratively, from a no-flux boundary condition. The flowfield on which this no-flux condition is applied is governed by a passage-averaged momentum analysis that couples the blade pressure boundary conditions to the prescribed flow turning distribution.

Despite the considerable success of Dang,[3] Dang and Isgro,[4] and Dang et al.[5] with this method, we have developed several new treatments that have allowed us to accelerate its convergence and enhance its accuracy. By describing a blade geometry as a mean camberline with a specified thickness distribution, we will show how this camberline can be obtained from a Lagrangian analysis that overlays the blade onto a material line convected from inflow to outflow. This treatment enhances both our calculation's global convergence and its spatial accuracy near leading and trailing edges. We will also show how a passage-averaged flow turning distribution can be used to derive an unsteady pressure boundary condition that also accelerates our calculations to a steady state.

II. Governing Equations

An inverse design technique requires that we develop a coupled system of equations from which to obtain both the geometry of interest and the flowfield around it. This is in contrast to an analysis method in which the flow around a known geometry is constructed.

A. Flow Equations

For an inviscid compressible flow in the Cartesian coordinate system (x, y), the conservation laws of continuity, linear momentum, and energy can be written as

$$\int \frac{\partial \boldsymbol{w}}{\partial t}\,\mathrm{d}\forall + \oint \bar{F}\cdot\boldsymbol{n}\,\mathrm{d}\sigma = 0 \tag{1}$$

where $\boldsymbol{w} = \{\rho, \rho u, \rho v, \rho E\}$, $\bar{F}\cdot\boldsymbol{e}_x = \{\rho u, \rho u^2 + p, \rho uv, u(E + p)\}$, ρ is density, p is pressure, (u, v) are Cartesian velocity components, E is the total energy, $\boldsymbol{n}$ is a surface normal, and $\mathrm{d}\forall$ and $\mathrm{d}\sigma$ are elemental volumes and surface areas, respectively.

B. Camberline Equation

We can define a turbomachinery blade geometry as

$$\alpha^{\pm} = y - (f \pm T/2) \tag{2}$$

where α^+ and α^- are the blade's upper and lower surfaces, $f = f(x)$ is the blade's camber line, and $T = T(x)$ is the blade's thickness distribution. If we then assume that the blade surfaces are material surfaces, we can write

$$\frac{\mathrm{D}\alpha^+}{\mathrm{D}t} = \frac{\mathrm{D}\alpha^-}{\mathrm{D}t} = 0 \tag{3}$$

which, when combined with Eq. (2), becomes

$$\frac{\partial f}{\partial t} + u^{\pm}\frac{\partial f}{\partial x} = \mp\frac{1}{2}u^{\pm}\frac{\mathrm{d}T}{\mathrm{d}x} + v^{\pm} \tag{4}$$

on the upper and lower surfaces, respectively. Finally, mimicking the steady analysis of Dang,[3] we can combine these two conditions to produce the equation

$$\frac{\partial f}{\partial t} + \frac{(u^+ + u^-)}{2}\frac{\partial f}{\partial x} = -\frac{(u^+ + u^-)}{4}\frac{\mathrm{d}T}{\mathrm{d}x} + \frac{(v^+ + v^-)}{2} \tag{5}$$

from which our camberline is obtained. This equation is an unsteady form of the camberline generating condition first proposed by Dang.[3] However, because we have constructed our camberline equation from a Lagrangian description and not a simple no-flux condition, our blade can be overlapped onto a material line that convects from inflow to outflow. In essence, inversely designing both our camberline and the stagnation streamlines upstream and downstream of the leading and trailing edges, respectively. The benefit of this approach is that we can then align our numerical grid along this material line to produce a locally one-dimensional resolution of the flow into and out of the leading- and trailing-edge regions, thus enhancing both the flow resolution near the leading and trailing edges and our steady-state convergence.

III. Numerical Approximation

The flow and camberline equations, Eqs. (1) and (5), are combined into a single nonlinear system that is then solved by the multistage scheme of Jameson et al.[6] The flow and camberline residuals are approximated by a finite volume formulation that constructs the fluxes on the faces of each mesh cell with a simple bilinear averaging.

Pressures along the blades' upper and lower surfaces are constructed from the following first-order Taylor series approximations:

$$p(f \pm T/2) = p(f) \pm \Delta p/2 \tag{6}$$

where $\Delta p = p(f + T/2) - p(f + S - T/2)$ is the pressure difference across the blade in the pitchwise direction and S is the blade spacing. This pressure difference is obtained by first integrating the pitchwise component of the linear momentum equation as follows:

$$\int_{f+T/2}^{f+S-T/2} \rho\frac{\mathrm{D}v}{\mathrm{D}t}\,\mathrm{d}y = -\int_{f+T/2}^{f+S-T/2}\frac{\partial p}{\partial y}\,\mathrm{d}y = \Delta p \tag{7}$$

Received 26 August 1998; revision received 11 May 2000; accepted for publication 18 May 2000.

*Associate Professor, Department of Mechanical Engineering. Senior Member AIAA.
‡Graduate Student, Department of Mechanical Engineering.

By defining the mass flux weighted, pitchwise-averaged flow turning

$$\bar{v} = \bar{v}(x) = \frac{1}{\dot{m}} \int_{f+T/2}^{f+S-T/2} \rho u v \, \mathrm{d}y \tag{8}$$

we can then differentiate this term in the x direction, assuming a constant mass flow, to obtain the mass flow weighted flow turning distribution

$$\dot{m}\frac{\mathrm{d}\bar{v}}{\mathrm{d}x} = \int_{f+T/2}^{f+S-T/2} \frac{\partial}{\partial x}(\rho u v)\,\mathrm{d}y + \rho u v \frac{\partial y}{\partial x}\bigg|_{f+S-T/2} - \rho u v \frac{\partial y}{\partial x}\bigg|_{f+T/2} \tag{9}$$

Evoking continuity and the camberline conditions [Eq. (2)], we can write

$$\Delta p = \dot{m}\frac{\mathrm{d}\bar{v}}{\mathrm{d}x} + \int_{f+T/2}^{f+S-T/2} \frac{\partial}{\partial t}(\rho v)\,\mathrm{d}y \tag{10}$$

where the blade's loading distribution is now the specified design criteria. Thus, the following unsteady numerical boundary condition is used:

$$\Delta p^{n+1} = \dot{m}\frac{\mathrm{d}\bar{v}}{\mathrm{d}x}\bigg|_{\text{input}} - \int_{f+T/2}^{f+S-T/2} \left\{ \frac{\partial}{\partial x}(\rho u v) + \frac{\partial}{\partial y}(\rho v^2 + p) \right\}^n \mathrm{d}y \tag{11}$$

where n identifies the time level, or iteration, of our approximation.

IV. Results

Numerical results are presented to illustrate both the convergence acceleration and the enhanced flow resolution produce by our new camberline model and unsteady pressure boundary conditions.

All of our calculations were performed on sheared H-type meshes whose vertical grid lines were aligned with the y axis. The numerical domain, typically a 128×32 cell grid with 64 mesh cells between the leading and trailing edges, was extended one chord upstream and downstream of the blade's leading and training edges, respectively. Grid lines were clustered near the leading and trailing edges with an algebraic stretching that placed the smallest mesh cells, a size of approximately 0.004 of a chord, adjacent to the blade's solid surfaces.

Our first test case was a low subsonic turbine designed to produce a mass flow of $\dot{m} = 0.352 p_0 c/\sqrt{(R)T_0}$ for specified back pressure of $p = 0.9 p_0$. Here, c is the blade's chord length, R is the gas constant, and p_0 and T_0 are the upstream stagnation pressure and temperature, respectively. The resulting blade was designed by specifying a spacing-to-chord ratio of unity. The loading distribution specified was the one most commonly attributed to Hawthorne et al.[1] and takes the form

$$\frac{\mathrm{d}\bar{v}}{\mathrm{d}x} = C x^a (1-x)^b \tag{12}$$

where $a = 1/4$ and $b = 7/4$ and C is obtained from

$$\Delta v = C \int_{x=le}^{x=te} x^a (1-x)^b \tag{13}$$

where the total turning, $\Delta\bar{v} = -0.25\sqrt{(R)T_0}$, is specified a priori. The inlet flow angle was set to zero, and the resulting blade design turns the flow a total of 33 deg. The specified thickness distribution was of the form

$$T(x) = k x^{\frac{1}{2}} (1-x)^{\frac{1}{2}} \tag{14}$$

where the scalar constant k is chosen to ensure that $T_{\max} = 0.25c$.

The resulting flowfield is fully subsonic and accelerates the flow from an inflow Mach number of approximately $M = 0.32$ to a downstream value of $M = 0.41$

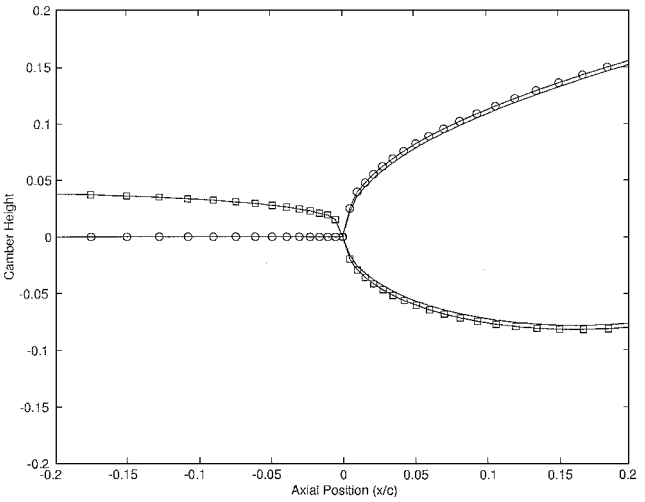

Fig. 1 Old and new camberline grids: ○, Dang's original scheme,[3] and ◇, modified technique.

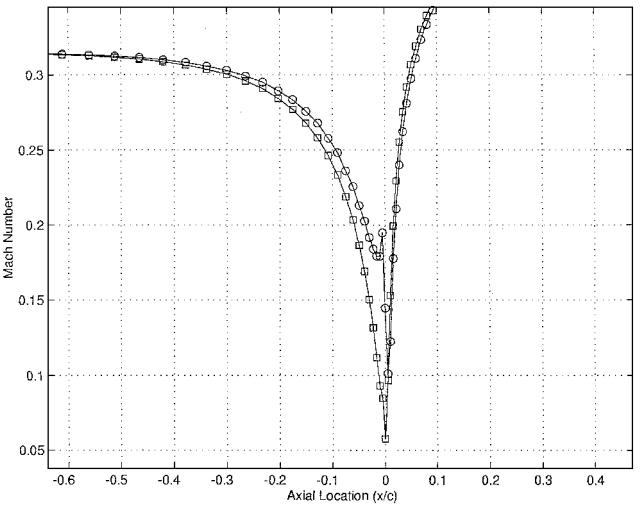

Fig. 2 Mach number distributions: ○, Dang's original scheme,[3] and ◇, modified technique.

With our new camberline treatment, the resulting grid lines are displaced vertically to match the path of a material quantity. Thus, the upstream grid lines mimic the path of a massless particle convected from the inflow boundary to the stagnation point on the leading edge. These effects can be seen in Fig. 1, where we have compared our new Lagrangian grid line to the grid obtained from Dang's original scheme,[3] one that simply follows the path along the inflow angle. With this treatment, our calculations increase in accuracy because the flow is locally one dimensional. The enhanced resolution near the leading edge can be seen in Fig. 2, where we have again compared the results from our Lagrangian camberline treatment to the ones obtained from Dang's original scheme,[3] where a static grid was used to follow the path of the inflow angle. Although both grids have the same horizontal and vertical clustering around their leading edges, the flow on the static grid is seen to be both discontinuous and oscillatory. Clearly, this stagnation flow is captured more accurately with our new camberline treatment.

Finally, our camberline treatment, when coupled with our unsteady pressure conditions, enhances significantly the convergence of our steady-state calculations. Shown in Fig. 3 is a comparison of the convergence histories, both with and without these new modifications. By the use of Dang's original scheme,[3] the maximum residual is reduced approximately 13 orders of magnitude within 60,000 iterations. With our new camberline and pressure boundary conditions, we can produce the same result in half

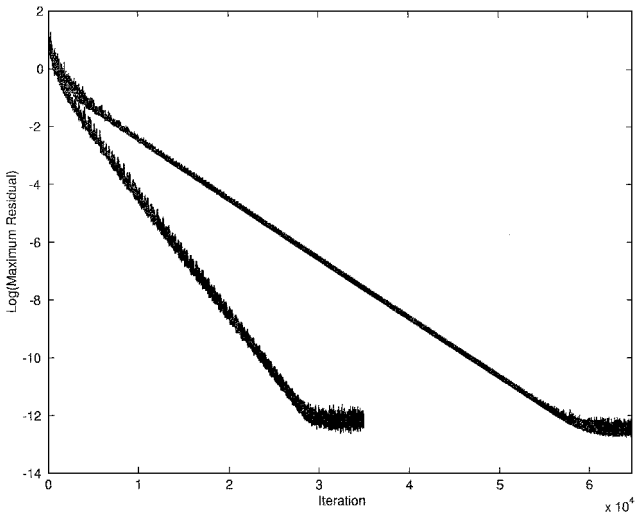

Fig. 3 Convergence histories.

the number of iterations, a significant reduction in computational work.

V. Conclusions

With this work we have presented several new ways to accelerate the convergence of an inverse design technique for constructing transonic turbomachinery cascades.

By describing a blade geometry as a mean camberline with a specified thickness distribution, we have shown how this camberline can be obtained from a Lagrangian analysis that overlays the blade onto a material line that convects from inflow to outflow. Numerical results were presented to illustrate the enhanced convergence acceleration and flow resolution that can be produced by this new approach.

We also showed how a passage-averaged flow turning distribution can be used to derive an unsteady pressure boundary condition to further accelerate our calculations to a steady state.

Acknowledgments

We are grateful to the Natural Sciences and Engineering Research Council of Canada (NSERC) for supporting this work under NSERC Grant OGP 170377. It is with pleasure that we acknowledge the numerous conversations held throughout the course of this work with T. Q. Dang and acknowledge his inverse design code on which our work is based.

References

[1]Hawthorne, W. R., Wang, C., Tan, C. S., and McCune, J. E., "Theory of Blade Design for Large Deflections, Part 1: Two-Dimensional Cascades," *Journal of Engineering for Gas Turbines and Power*, Vol. 106, No. 2, 1984, pp. 346–353.

[2]Tan, C. S., Hawthorne, W. R., McCune, J. E., and Wang, C., "Theory of Blade Design for Large Deflections, Part II: Two-Dimensional Cascades," *Journal of Engineering for Gas Turbines and Power*, Vol. 106, No. 2, 1984, pp. 354–365.

[3]Dang, T. Q., "Inverse Method for Turbomachine Blades Using Shock-Capturing Techniques," AIAA Paper 95-2465, 1995.

[4]Dang, T., and Isgro, V., "Euler-Based Inverse Method for Turbomachine Blades Part 1: Two-Dimensional Cascades," *AIAA Journal*, Vol. 33, No. 12, 1995, pp. 2309–2315.

[5]Dang, T. Q., Nerurkar, A. C., and Reddy, D. R., "Design Modification of Rotor 67 by 3D Inverse Method-Inviscid Flow Limit," American Society of Mechanical Engineers, Paper 97-GT-484, 1997.

[6]Jameson, A., Schmidt, W., and Turkel, E., "Numerical Solutions of the Euler Equations by Finite Volume Methods Using Runge–Kutta Time-Stepping Schemes," AIAA Paper 81-1259, 1981.

A. Plotkin
Associate Editor

Studies on Polygonal Slot Jets

K. Srinivasan*
Indian Institute of Technology, Guwahati 781 001, India
and
E. Rathakrishnan†
Indian Institute of Technology, Kanpur 208 016, India

Introduction

JET mixing finds application in a variety of flow systems such as combustion chambers, high-pressure valves, propulsive systems, etc. Jet mixing problems assume higher dimensions at high speeds due to compressibility effects and the presence of shocks. Passive control mechanisms have been attractive in effectively dealing with these problems. In this regard, noncircular jets are promising due to their efficacy in mixing and noise suppression. Among the noncircular jets, polygonal jets combine the advantage of streamwise vortices generated at the sharp corners and the large-scale structures rolling up from the flat surfaces. Such a combination is attractive because high-performance combustors and propulsive systems require both large-scale and fine-scale mixing. Many investigators have studied triangular jets[1–3] and rectangular jets[4–10] from different points of view. However, polygonal jets with more than four sharp corners have not been studied exhaustively. There are, however, studies on certain complex polygonal shapes such as cruciform configurations available in the literature.[11,12]

In this Note, flow characteristics of jets from polygonal slots have been investigated. Four regular polygonal slots (triangular, square, pentagonal, and hexagonal) are considered. The equivalent diameter D_e (diameter of a circle having the same area) of the slots is 10 mm. Jet issuing from slots made on thin plates are used, rather than contoured nozzles, to ensure azimuthal uniformity in the boundary-layer growth to enable a proper comparison of different geometries.[13] Furthermore, in some practical applications, expeditious manufacturing and ease of installation may dictate the use of sharp-edged slots in preference to nozzles with contoured upstream shaping.[12,14]

Details of Experiments

The experiments were carried out at the high-speed jet test facility, shown schematically in Fig. 1, of the Indian Institute of Technology, Kanpur. Different exit Mach numbers are achieved by varying the settling chamber (stagnation) pressure P_0. Circular plates of 1.5-mm thickness, over which slots of required geometry were made, were attached to the disk holder. The area ratio between the slot holder pipe and the slot was 100. The slots were flat (square) edged. The flattened edges of the slots were uniformly smooth. The centroid of the slot was chosen to be the origin in the present study (see Fig. 1).

Tests were conducted on jets issuing at several subsonic Mach numbers M_j ranging from 0.2 to 1.0 to obtain the flow characteristics. The pitot pressure was used to obtain the velocities using the isentropic relation

$$M_j = \sqrt{5\left[(P_a/P_t)^{-0.2857} - 1\right]} \tag{1}$$

where P_t and P_a are the pitot and ambient pressures, respectively. From the velocity profiles, half widths $Y_{0.5}$ and $Z_{0.5}$ were calculated. The pitot pressures were measured using a probe of 0.6-mm outer diameter and 0.4-mm inner diameter, designed according to recommendations by Nagai.[15] The flowfield was captured by pitot probe survey using a three-way traversing system. The pitot probe was connected to a PSI 9010 multichannel pressure transducer in

Received 27 September 1999; presented as Paper 2000-0613 at the AIAA 38th Aerospace Sciences Meeting, Reno, NV, 10–13 January 2000; revision received 4 April 2000; accepted for publication 11 May 2000.

*Assistant Professor, Department of Mechanical Engineering.
†Professor, Department of Aerospace Engineering.